University of Guayaquil

Faculty of Chemical engineering

INQUIDE
Chemical Engineering and Development
https://revistas.ug.edu.ec/index.php/iqd

e-ISSN: 3028-8533 / INQUIDE / Vol. 07 / Nº 02

INQUIDE
Ingeniería Química y Desarrollo

Thermo-hydraulic design of a finned tube double-pipe heat exchanger for acetone cooling.

Diseño térmico-hidráulico de un intercambiador de calor de doble tubo aleteado para el enfriamiento de acetona.

Amaury Pérez Sánchez [1] *; Elizabeth Elianne Artigas Cañizares [2] ; Laura Thalia Alvarez Lores [3] ; Elizabeth Ranero González [4] & Eddy Javier Pérez Sánchez [5]

Received: 21/11/2024 – Accepted: 03/02/2025 – Published: 01/07/2025

Research Articles [X] Review Articles [ ] Essay Articles [ ]

* Corresponding author.

Abstract.
Finned tube double-pipe counter-flow heat exchangers are considered very effective, valuable and advantageous in the heat transfer industry. In the present paper a finned tube double pipe heat exchanger was designed applying a well-known design methodology, in order to cool down 2 kg/s of an acetone stream from 90 ºC to 30 ºC using chilled water available at 5 ºC. Several important design parameters were determined like the cleanliness factor and the number of hairpins, as well as the pressure drop and pumping power of both streams, among others. The heat load had a value of 276,030 W, while a mass flowrate of chilled water of 3.30 kg/s will be needed to cool the acetone stream. Both fluids will flow under turbulent regime inside the heat exchanger. The value of the cleanliness factor was 0.359, and about three hairpins will be needed. The pressure drop of both fluids are below the maximum value established by the heat exchange service, while the chilled water and acetone streams will need a pumping power of 3,662 W and 575 W, respectively.

Keywords.
Double pipe heat exchanger, finned tube, number of hairpins, pressure drop, pumping power.

Resumen.
Los intercambiadores de calor de flujo a de doble tubo aleteados a contracorriente son considerados muy efectivos, valiosos y ventajosos en la industria de la transferencia de calor. En el presente artículo un intercambiador de calor de doble tubo aleteado fue diseñado aplicando una metodología de diseño bien conocida, con el fin de enfriar 2 kg/s de una corriente de acetona desde 90 ºC hasta 30 ºC usando agua fría disponible a 5 ºC. Varios parámetros de diseño importantes fueron determinados tales como el factor de limpieza y el número de horquillas, así como también la caída de presión y potencia de bombeo de ambas corrientes, entre otros. La carga de calor tuvo un valor de 276 030 W, mientras que se necesitará un caudal másico de agua fría de 3,30 kg/s para enfriar la corriente de acetona. Ambos fluidos fluirán bajo régimen turbulento dentro del intercambiador de calor. El valor del factor de limpieza fue de 0,359, y se necesitarán alrededor de tres horquillas. La caída de presión de ambos fluidos está por debajo del valor máximo establecido por el servicio de transferencia de calor, mientras que las corrientes de agua fría y acetona necesitarán una potencia de bombeo de 3 662 W y 575 W, respectivamente.

Palabras clave.
Intercambiador de calor de doble tubo, tubo aleteado, número de horquillas, caída de presión, potencia de bombeo.

1. Introduction.

With the development of know-how, the significance of heat transfer engineering has boosted and there is a permanently need to encounter new design challenges to increase the performance and efficacy of the heat transfer field, particularly due to energy saving interests. Usually, heat exchangers are widely used for this purpose [1].

Heat exchangers are devices operated in numerous industries for heat transfer among fluids. Of the several types of heat exchangers that are utilized at industrial scale, possibly the two most significant are the double pipe and the shell and tube. Despite the fact that shell and tube heat exchangers generally provide greater surface area for heat transfer with a more compact design, greater ease of cleaning, and less probability of leakage, the double pipe heat exchanger (DPHE) still finds use in practice today [2].

One of the heat exchangers that have attracted the attention of researchers and engineers is the DPHE due to simplicity, effectiveness and wide range of usages [3].

[1] University of Camagüey; Faculty of Applied Sciences; amaury.perez84@gmail.com; https://orcid.org/0000-0002-0819-6760, Camagüey; Cuba.
[2] University of Camagüey; Faculty of Applied Sciences; elizabeth.artigas@reduc.edu.cu; https://orcid.org/0009-0003-3416-1355, Camagüey; Cuba.
[3] University of Camagüey; Faculty of Applied Sciences; laura.alvarez@reduc.edu.cu; https://orcid.org/0009-0007-2643-018X, Camagüey; Cuba.
[4] University of Camagüey; Faculty of Applied Sciences; eliza.eddy2202@gmail.com; https://orcid.org/0000-0001-9755-0276, Camagüey, Cuba.
[5] Company of Automotive Services S.A.; Commercial Department; eddyjavierpsanchez@gmail.com; https://orcid.org/0000-0003-4481-1262, Ciego de Ávila, Cuba.

A DPHE is a distinctive type of heat exchanger with two concentric pipes, one inside the other. There are two different fluid flows in a DPHE, such that one fluid flows inside the inner pipe and the other fluid flows in the annulus region outside of the inner pipe [4]. It involves two concentric pipes, two connecting tees, a return head, a return feed, and packing glands that support the inner pipe within the outer pipe (Figure 1). Each of two fluids −hot and cold− flow either through the inside of the inner pipe or through the annulus formed between the outside of the inner pipe and the inside of the outer pipe [2].

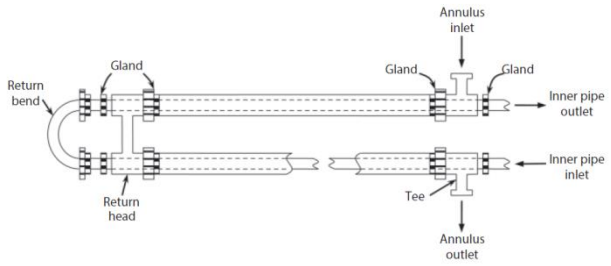

Fig. 1. Double pipe heat exchanger.
Source: [2].

DPHE have been utilized in the chemical processing industry for over 100 years. The first patent on this unit appeared in 1923 [2]. They are applied in several industrial processes and research areas; for example in waste heat recovery, for heating/cooling in chemical processes, as well as in the food industry to pasteurize/preheat liquid products (juices, mashes, jelly, etc.).

The DPHE is particularly convenient because it can be connected in any pipe-fitting shop from standard parts and offers an economical heat-transfer surface. The flow arrangement in this heat exchanger could be countercurrent or parallel (co-current). In countercurrent arrangement, the fluid in the pipe flows in a direction reverse to the fluid in the annulus. In parallel arrangement, the two fluids flow in the same direction. The variations of fluid temperature within the heat exchanger depend on whether the flow is parallel or countercurrent [2].

The main application of the DPHE is for sensible heating or cooling of process fluids where small heat transfer areas (up to 50 m^2) are necessary. This heat exchanger is also very appropriate for handling fluids with high pressure, because of the smaller diameter of the pipes. The major disadvantage is that they are bulky and expensive per unit of heat transfer surface area [5].

Although this unit is not extensively employed in industry (the heat transfer area is small relative to other heat exchangers), it serves as an excellent starting point from an academic and/or training perspective [2].

According to [6], if the stream contains solids in suspension, DPHEs may also be a better alternative, because they can be built with an inner tube with larger diameter to avoid plugging. Smaller diameters of the outer tube in DPHEs are effective for high-pressure applications, because it involves a smaller wall thickness. In addition, DPHEs may be easily cleaned, and the longitudinal flow avoids the existence of stagnation regions, which in shell and tube exchangers may cause fouling and corrosion. DPHEs have also the advantage of robustness due to its modular structure, which permits an easier adaptation to process adjustments.

Growing need to develop and improve the effectiveness of heat exchangers has led to a broad range of investigations for increasing heat transfer rate along with decreasing the size and cost of the industrial apparatus accordingly [3]. The enhancement of heat transfer has become an important factor in achieving these goals and has captured the interest of many researchers [7].

Enhancement of heat transfer in heat exchangers can be accomplished through two techniques [7]:
1. Increasing the convection coefficient. The convection coefficient may be improved by increasing turbulence, creating secondary flow, and inducing swirl flow. One or more of these mechanisms may be accomplished using coil-spring wire, ribs, indentation, spiral flutes transverse-ribbed tubes, helically ribbed tubes, wire-coil insert, twisted-tape insert, ribbed or ribbed grooved walls. Also, the convective heat transfer coefficient may be enhanced using fluids that experience a phase transition or by using electrohydrodynamic enhancement tools and employing mist flow.
2. Expanding the heat transfer area by employing longitudinal fins, wire-on-tube heat exchangers.
Other techniques apply both effects. Examples of these techniques are spiral fins or ribs and offset strip fins.

According to [4] the performance of heat exchangers can be enhanced by adopting appropriate procedures. These procedures comprise the implementation of extended surfaces, surface vibration, rough surfaces, and coiled tubes. Other authors [7] numerically investigated the effect of inserting porous substrates at both sides of the wall that separates the cold and hot working fluids on the performance of a conventional concentric tube heat exchanger.

Thermal systems are currently amongst the most dynamic technical systems. Numerous methods have been explored and tested in order to increase heat transfer in these systems and accomplish a high level of thermal performance. By exploiting a number of surface-enhancement-based approaches, the heat transfer rate of conventional heat exchangers may be improved. This development in heat transfer rate results from the conditions provided by the use of enhanced surfaces. These conditions prevent the

formation of the boundary layer, improve the turbulence level, increase the heat transfer area, and generate swirling and/or secondary flows. Enhanced heat transfer surfaces have several objectives for their use, being the most important to reduce the size of heat exchangers, which could lead to a decrease in their costs. In addition, they reduce the pumping power that is needed for specific thermal exchange processes, and improve the heat transfer coefficient. In turn, this increases the effectiveness and efficiency of thermal processes and results in operating cost savings [8].

Recently, several researchers have investigated ways to enhance heat transfer using the passive way in double-pipe heat exchangers (DPHE), such as using twisted strips, extended surfaces or fins, wired coils, and other turbulence-generating tools [9].

The use of solid fins to boost the heat transfer rates between two different fluids in tubular heat exchangers is one of the most successful and extensively applied approaches. Finned tubes are one of the most commonly used ways of passively enhancing the heat transfer in circular tube. They are applied to decrease the size of a heat exchanger required for a specified heat duty, or to increase heat transfer rate of an existing heat exchanger design. An internally finned tube can substantially increase the surface area, and can significantly augment the heat transfer rate. Finned tubes perform differently depending on whether the flow is laminar or turbulent. For both laminar and turbulent flow regimes, the finned tubes exhibit significantly higher heat transfer coefficients when contrasted with the corresponding smooth tubes. The performance of finned pipe is mainly determined by the type of flow, fin efficiency (which determines the average heat transfer coefficient) and the friction factor, which is responsible for pressure/pumping loss [10].

The use of a finned tube to increase heat transmission is becoming more important in a growing number of industrial applications; thus, the finned tube has been the subject of several studies [8]. In this context, [9] investigated the convection heat transfer in a countercurrent double-tube heat exchanger with a curved rectangular fin and rectangular fin in a turbulent flow using water-Al_2O_3 and water-TiO_2 nanofluids. Also, in [11] the enhancement of the thermal performance of the phase change material in a double-tube heat exchanger using new grid annular fins was investigated. In this study, the grid annular fins, which consisted of straight and circular strip components, were located on the inner tube. In another study, [8] carried out a numerical investigation of heat transfer enhancement in a double pipe heat exchanger embedded with an extended surface on the inner tube's outer surface with the addition of Alumina nanofluid and by using computational fluid dynamics (CFD) simulation. This investigation was carried out at Reynolds numbers ranging from 250 to 2,500 with an inner diameter of 20.4 mm. while the effect of the inner pipe's U fins' geometry on pressure drop, temperature distribution, and thermal performance was also scrutinized. Moreover, [12] carried out the numerical examination of heat transfer enhancement in individual annular serrated fins double tube heat exchanger, concluding that the maximum value of Nusselt number and maximal skin friction coefficient was found in 14 serrated fins. Besides, [4] studied the characteristics of convective heat transfer in the annular region of a finned DPHE with an innovative diamond-shaped fin design. The diamond-shaped fins are longitudinally increased on the outer surface of the inner pipe of the DPHE. The arrangement of the diamond-finned annulus was verified by the numerous values of the geometrical parameters, such as the radii ratio, fins number, fin-height, and fin thickness. The effects of these variables on various performance parameters, such as the product of the Reynolds number and friction factor, Nusselt number, and j-factor, were computed. The type of fin evaluated in this study was considered for the first time in the design of DPHEs. In [10] a simple semi-empirical-numerical methodology to evaluate heat transfer and pressure drop characteristics in a finned tube heat exchanger with internal and/or external fins was described, which can be applied in a wide range of operating conditions of practical importance. In [3] the thermo hydraulic performance of a proposed design of an air-to-water double pipe heat exchanger with helical fins on the annulus gas side was numerically studied. Three-dimensional CFD simulations were implemented, using the FLUENT software with the aim of examine the gas side fluid flow, turbulence, heat transfer, and power consumption for different arrangements of the heat exchanger. Moreover, [13] carried out various experiments to investigate and compare the heat transfer in a DPHE for counter flow arrangement with and without usage of longitudinal triangular fins. Triangular fins with dimensions of 9 mm base, 8 mm height and 2 mm thickness were applied in this study. Other authors [6] investigated the design optimization of a DPHE using mathematical programming. The heat exchanger area is decreased and the thermo-fluid dynamic settings are considered for the application of the right transport equations, together with design conditions, such as maximum pressure drops and minimum excess area. The modular structure of this heat exchanger type and the allocation of the streams (inside the inner tube or in the annulus) are also considered. Two mixed-integer nonlinear programming (MINLP) approaches were also purported. Likewise, [14] aimed to develop new designs of DPHE to improve the heating/cooling processes at the lowest possible pumping power. Consequently, the thermal performance analysis of three configurations of DPHE was implemented. The studied arrangements were circular wavy DPHE, plain oval DPHE and an oval wavy DPHE. In addition, the conventional DPHE was utilized as a reference heat exchanger, and a validated CFD approach was executed to perform this study. In [15], the helical fins effect in the performance of a water-air DPHE was examined

experimentally. The performance in terms of average heat transfer rate, heat transfer coefficient and effectiveness of heat exchanger in plain inner pipe (without helical fin) was assessed and contrasted with a heat exchanger having helical fins installed over inner pipe. In [1], the analysis of fully developed laminar convective heat transfer in an innovated design of a finned DPHE with longitudinal fins of variable thickness of the tip subjected to the constant heat transfer rate boundary conditions was investigated. In this study, the overall performance of the proposed DPHE was examined by taking into account the friction factor, the Nusselt number and the j-factor. Finally, [16] aimed at comparison of heat transfer characteristics using different fin profiles for a DPHE under various operating conditions to evolve with the best possible configuration. The selected configurations in this study were rectangular, triangular and concave parabolic. Base width, height and number of fins were held identical to be specifically compared. Numerical simulation was completed using commercial CFD software. Several particular heat transfer parameters like temperature deviation, heat transfer rate, heat transfer coefficient and fin effectiveness for the models mentioned above were compared and shown.

The addition of porous material as an alternative method to improve heat exchange in these thermal equipment seems to be promising. In this sense, [17] investigated the heat transfer enhancement when porous fins are attached at the inner cylinder of a DPHE. This arrangement is selected in order to augment the heat transfer surface area between the fins and the cold fluid to be heated. The influence of several parameters such as Darcy number, the height and spacing of fins and the thermal conductivity ratio on the hydrodynamic and thermal fields were also investigated.

Liquid acetone is produced in a chemical processing plant, and it's desired to cool down this liquid acetone stream from 90 ºC to 30 ºC, using chilled water available at 5 ºC. To accomplish this heat exchange operation, a finned tube double pipe heat exchanger has been proposed due to space availability and limited budget. Thus, the present paper aimed to design a finned tube DPHE both from the thermal and hydraulic points of view, using the methodology and correlations reported in [5] and [18], where several important design parameters were determined such as the cleanliness factor and the total number of hairpins, as well as the pressure drop and pumping power of both streams.

2. Materials and methods.

2.1. Problem definition.

It's required to cool 2 kg/s of an acetone stream from 90 ºC to 30 ºC using chilled water at 5 ºC. The chilled water outlet temperature must not be higher than 25 ºC. The following initial parameters are available (Figure 2):

- Length of hairpin (L_t): 4.2 m.
- Nominal diameter of annulus: 2 in.
- Nominal diameter of inner tube: ¾ in.
- Fin height (H_f): 0.0125 m
- Fin thickness (δ): 0.9 mm.
- Number of fins per tube (N_f): 28.
- Material: Carbon steel.
- Thermal conductivity of carbon steel (k_m): 52 W/m.K [5].
- Number of tubes inside the annulus (N_t): 1.

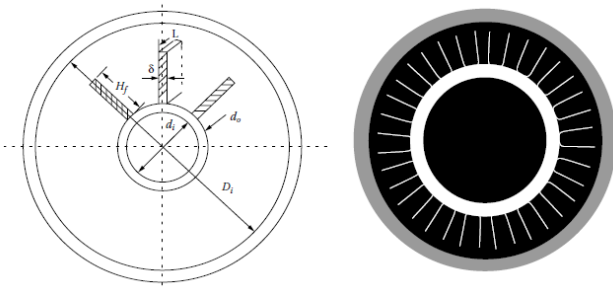

Fig. 2. Cross section of a longitudinally finned inner tube heat exchanger and nomenclature of the initial parameters.
Source: [5].

According to [5] the fouling factors for acetone and water are 0.000352 and 0.000176 m^2.K/W respectively. It's preferred that both streams flow under countercurrent arrangement in the designed heat exchanger, while the pressure drop of the acetone and chilled water must not exceed 200,000 Pa and 900,000 Pa, respectively. Calculate the surface area and the number of hairpins of the heat exchanger, as well as the pressure drops and pumping power for both streams.

2.2. Number of hairpins.

Step 1. Definition of the initial parameters.
Step 2. Diameters of both the inner tube and annulus.
Step 3. Average temperature of both fluids:

- Hot fluid:

$$\overline{T} = \frac{T_1 + T_2}{2} \quad (1)$$

- Cold fluid:

$$\bar{t} = \frac{t_1 + t_2}{2} \quad (2)$$

Step 4. Physical properties of both fluids at the average temperature of the previous step.
Table 1 shows the physical properties that must be defined for both fluids at the average temperature calculated in the previous step.

Table 1. Physical properties of both fluids

Physical property	Acetone	Chilled water	Units
Density	ρ_h	ρ_c	kg/m^3
Viscosity	μ_h	μ_c	Pa.s
Thermal conductivity	k_h	k_c	W/m.K
Heat capacity	Cp_h	Cp_c	J/kg.K

Source: Own elaboration.

Step 5. Heat load (Q):

$$Q = m_h \cdot Cp_h \cdot (T_1 - T_2) \quad (3)$$

Step 6. Mass flowrate of chilled water (m_c):

$$m_c = \frac{Q}{Cp_c \cdot (t_2 - t_1)} \quad (4)$$

Step 7. Location of the fluids inside the heat exchanger.

Step 8. Net cross-sectional area in the annulus with longitudinal finned tubes (A_c):

$$A_c = \frac{\pi}{4} \cdot (D_i^2 - d_o^2 \cdot N_t) - \delta \cdot H_f \cdot N_t \cdot N_f \quad (5)$$

Step 9. Total wetted perimeter of the annulus with longitudinally finned inner tubes (P_w):

$$P_w = \pi \cdot (D_i + d_o \cdot N_t) + 2 \cdot H_f \cdot N_f \cdot N_t \quad (6)$$

Step 10. Hydraulic diameter (D_h):

$$D_h = \frac{4 \cdot A_c}{P_w} \quad (7)$$

Step 11. Heat transfer perimeter of the annulus for heat transfer (P_h):

$$P_h = (\pi \cdot d_o + 2 \cdot H_f \cdot N_f) \cdot N_t \quad (8)$$

Step 12. Equivalent diameter for heat transfer (D_e):

$$D_e = \frac{4 \cdot A_c}{P_h} \quad (9)$$

Step 13. Velocity of the tube side fluid (u_t):

$$u_t = \frac{m_t}{\rho_t \cdot \frac{\pi \cdot d_i^2}{4}} \quad (10)$$

Step 14. Reynolds number of the tube side fluid (Re_t):

$$Re_t = \frac{\rho_t \cdot u_t \cdot d_i}{\mu_t} \quad (11)$$

Step 15. Prandtl number of the tube side fluid (Pr_t):

$$Pr_t = \frac{Cp_t \cdot \mu_t}{k_t} \quad (12)$$

Step 16. Nusselt number of the tube side fluid (Nu_t):

- Laminar regime (Re_t < 2,300):

Temperature of the tube wall (T_w):

$$T_w = 0.5 \cdot (\bar{T} - \bar{t}) \quad (13)$$

Viscosity of the tube side fluid (μ_t) and water (μ_w) at T_w.

Nusselt number of the tube side fluid under laminar flow:

$$Nu_t = 1.86 \cdot \left(Re_t \cdot Pr_t \cdot \frac{d_i}{L_t}\right)^{1/3} \cdot \left(\frac{\mu_t}{\mu_w}\right)^{0.14} \quad (14)$$

- Transition regime (2,300 ≤ Re_t ≤ 10,000):

$$\frac{h_t}{Cp_t \cdot \rho_t \cdot u_t} = 0.116 \cdot \left(\frac{Re_t^{0.66} - 125}{Re_t}\right) \cdot \left[1 + \left(\frac{d_i}{L_t}\right)^{0.66}\right] \cdot Pr_t^{-0.66} \quad (15)$$

- Turbulent regime (10,000 < Re_t < 5,000,000):

Friction factor (f_t):

$$f_t = (1.58 \cdot lnRe_t - 3.28)^{-2} \quad (16)$$

Nusselt number (Nu_t):

$$Nu_t = \frac{\left(\frac{f_t}{2}\right) \cdot Re_t \cdot Pr_t}{1.07 + 12.7 \cdot \left(\frac{f_t}{2}\right)^{1/2} \cdot (Pr_t^{2/3} - 1)} \quad (17)$$

Step 17. Convective heat transfer coefficient of the tube side fluid (h_t):

$$h_t = \frac{Nu_t \cdot k_t}{d_i} \quad (18)$$

Step 18. Velocity of the annulus fluid (u_a):

$$u_a = \frac{m_a}{\rho_a \cdot A_c} \quad (19)$$

Step 19. Reynolds number of the annulus fluid (Re_a):

$$Re_a = \frac{\rho_a \cdot \mu_a \cdot D_h}{\mu_a} \quad (20)$$

Step 20. Prandtl number of the annulus fluid (Pr_a):

$$Pr_a = \frac{Cp_a \cdot \mu_a}{k_a} \quad (21)$$

Step 21. Nusselt number of the annulus fluid (Nu_a):

- Laminar regime (Re_a < 2,300):

Viscosity of the annulus fluid (μ_a) at T_w.

Nusselt number of the annulus fluid:

$$Nu_a = 1.86 \cdot \left(Re_a \cdot Pr_a \cdot \frac{D_h}{L_t}\right)^{1/3} \cdot \left(\frac{\mu_a}{\mu_w}\right)^{0.14} \quad (22)$$

- Transition regime (2,300 ≤ Re_a ≤ 10,000):

$$\frac{h_t}{Cp_a \cdot \rho_a \cdot u_a} = 0.116 \cdot \left(\frac{Re_a^{0.66} - 125}{Re_a}\right) \cdot \left[1 + \left(\frac{D_h}{L_t}\right)^{0.66}\right] \cdot Pr_a^{-0.6} \quad (23)$$

- Turbulent regime (10,000 < Re_a < 5,000,000):

Friction factor (f_a):

$$f_a = (1.58 \cdot lnRe_a - 3.28)^{-2} \quad (24)$$

Nusselt number (Nu_a):

$$Nu_t = \frac{\left(\frac{f_a}{2}\right) \cdot Re_a \cdot Pr_a}{1.07 + 12.7 \cdot \left(\frac{f_a}{2}\right)^{1/2} \cdot \left(Pr_a^{2/3} - 1\right)} \quad (25)$$

Step 22. Convective heat transfer coefficient of the annulus fluid (h_a):

$$h_a = \frac{Nu_a \cdot k_a}{D_e} \quad (26)$$

Step 23. Finned heat transfer area (A_f):

$$A_f = 2 \cdot N_t \cdot N_f \cdot L_t \cdot (2 \cdot H_f + \delta) \quad (27)$$

Step 24. Unfinned heat transfer area (A_u):

$$A_u = 2 \cdot N_t \cdot (\pi \cdot d_o \cdot L_t - N_f \cdot L_t \cdot \delta) \quad (28)$$

Step 25. Total area of hairpin (A_t):

$$A_t = A_f + A_u \quad (29)$$

Step 26. Factor m:

$$\mathrm{m} = \sqrt{\frac{2 \cdot h_a}{\delta \cdot k_m}} \quad (30)$$

Step 27. Fin efficiency (η_f):

$$\eta_f = \frac{tanh(m \cdot H_f)}{m \cdot H_f} \quad (31)$$

Step 28. Overall surface efficiency (η_o):

$$\eta_o = \left[1 - (1 - \eta_f) \cdot \frac{A_f}{A_t}\right] \quad (32)$$

Step 29. Area of the inner tube (A_i):

$$A_i = 2 \cdot \pi \cdot d_i \cdot L_t \quad (33)$$

Step 30. Overall heat transfer coefficient under fouled conditions (U_f):

$$U_f = \frac{1}{\frac{A_t}{A_i} \cdot \frac{1}{h_t} + \frac{A_t}{A_i} \cdot R_t + \frac{A_t \cdot ln\left(\frac{d_o}{d_i}\right)}{2 \cdot \pi \cdot k_m \cdot 2 \cdot L_t} + \frac{R_a}{\eta_o} + \frac{1}{\eta_o.h}} \quad (34)$$

Step 31. Overall heat transfer coefficient under clean conditions (U_c):

$$U_c = \frac{1}{\frac{A_t}{A_i} \cdot \frac{1}{h_t} + \frac{A_t \cdot ln\left(\frac{d_o}{d_i}\right)}{2 \cdot \pi \cdot k_m \cdot 2 \cdot L_t} + \frac{1}{\eta_o.h_a}} \quad (35)$$

Step 32. Cleanliness factor (CF):

$$\mathrm{CF} = \frac{U_f}{U_c} \quad (36)$$

Step 33. Log-mean temperature difference (LMTD) (for countercurrent flow):

$$\mathrm{LMTD} = \frac{(T_1 - t_2) - (T_2 - t_1)}{ln\frac{(T_1 - t_2)}{(T_2 - t_1)}} \quad (37)$$

Step 34. Total heat transfer surface area without fouling (A_{oc}):

$$A_{oc} = \frac{Q}{U_c \cdot LMTD} \quad (38)$$

Step 35. Total heat transfer surface area with fouling (A_{of}):

$$A_{of} = \frac{Q}{U_f \cdot LMTD} \quad (39)$$

Step 36. Number of hairpins (N_h):

$$N_h = \frac{A_{of}}{A_t} \quad (40)$$

2.3. Pressure drop.

Step 37. Friction factor of the tube side fluid (f_t'):

- Laminar regime (Re_t < 2,300):

$$f_t = \frac{16}{Re_t} \quad (41)$$

Friction factor of the tube side fluid under laminar flow:

$$f_t' = f_t \cdot \left(\frac{\mu_t}{\mu_w}\right)^{-0.58} \quad (42)$$

- Turbulent regime (4,000 < Re_t < 5,000,000):

$$f_t' = 0.00140 + 0.125 \cdot Re_t^{-0.32} \quad (43)$$

Step 38. Pressure drop of the tube side fluid (Δp_t):

$$\Delta p_t = 4 \cdot f_t' \cdot \frac{2 \cdot L_t}{d_i} \cdot \rho_t \cdot \frac{u_t^2}{2} \cdot N_h \quad (44)$$

Step 39. Friction factor of the annulus fluid (f_a'):

- Laminar regime (Re_a < 2,300):

$$f_a = \frac{16}{Re_a} \quad (45)$$

Friction factor of the annulus fluid under laminar flow:

$$f_a' = f_a \cdot \left(\frac{\mu_a}{\mu_w}\right)^{-0.58} \quad (46)$$

- Turbulent regime (4,000 < Re_a < 5,000,000):

$$f_a' = 0.00140 + 0.125 \cdot Re_a^{-0.32} \quad (47)$$

Step 40. Pressure drop of the annulus fluid (Δp_a):

$$\Delta p_a = 4 \cdot f_a' \cdot \frac{2 \cdot L_t}{D_h} \cdot \rho_a \cdot \frac{u_a^2}{2} \cdot N_h \quad (48)$$

2.4. Pumping power.

Step 41. Pumping power required for the tube side fluid (P_t):

$$P_t = \frac{m_t \cdot \Delta p_t}{\rho_t \cdot \eta_p} \quad (49)$$

Where η_p is the pump efficiency = 0.80 - 0.85 [5].

Step 42. Pumping power required for the annulus fluid (P_a):

$$P_a = \frac{m_a \cdot \Delta p_a}{\rho_a \cdot \eta_p} \quad (50)$$

3. Results.

The values of the main design parameters calculated for the proposed finned tube double-pipe heat exchanger are shown hereafter, which include the calculated number of hairpins, as well as the pressure drop and pumping power for both streams.

3.1. Number of hairpins.

Step 1. Definition of the initial parameters:
Table 2 shows the initial parameters which are required to design the double-pipe heat exchanger.

Table 2. Initial parameters available.

Parameters	Symbol	Value	Units
Mass flowrate of acetone	m_h	2.00	kg/s
Inlet temperature of acetone	T_1	90	ºC
Outlet temperature of acetone	T_2	30	ºC
Inlet temperature of water	t_1	5	ºC
Outlet temperature of water	t_2	25	ºC
Fouling factor of acetone	R_h	0.000352	m².K/W
Fouling factor of water	R_c	0.000176	m².K/W
Maximum pressure drop for acetone	Δp_{hm}	200,000	Pa
Maximum pressure drop for water	Δp_{cm}	900,000	Pa

Source: Own elaboration.

Step 2. Diameters of both the inner tube and annulus.
Presented next are the values of the inner and outer diameters for an inner tube with a nominal diameter of ¾ Schedule 40, and also the outer diameter for an annulus with a nominal diameter 2 Schedule 40, as reported by [19].

- Inner diameter of tube (d_i) = 0.02093 m.
- Outer diameter of tube (d_o) = 0.02667 m.
- Inner diameter of annulus (D_i) = 0.0525 m.

Step 3. Average temperature of both fluids:

- Acetone:

$$\bar{T} = \frac{T_1 + T_2}{2} = \frac{90 + 30}{2} = 60\ ℃ \quad (1)$$

- Water:

$$\bar{t} = \frac{t_1 + t_2}{2} = \frac{5 + 25}{2} = 15\ ℃ \quad (2)$$

Step 4. Physical properties of both fluids at the average temperature of the previous step.
Table 3 displays the values of the physical properties for both fluids, which were determined according to data reported in [19].

Table 3. Physical properties of both fluids.

Physical property	Acetone	Chilled water	Units
Density	745.20	999.10	kg/m³
Viscosity	0.000229	0.00114	Pa.s
Thermal conductivity	0.146	0.589	W/m.K
Heat capacity	2,300.25	4,188.47	J/kg.K

Source: Own elaboration.

Step 5. Heat load (Q):

$$Q = m_h \cdot Cp_h \cdot (T_1 - T_2) \quad (3)$$

$$Q = 2.00 \cdot 2{,}300 \cdot (90 - 30) = 276{,}030\ W$$

Step 6. Mass flowrate of chilled water (m_c):

$$m_c = \frac{Q}{Cp_c \cdot (t_2 - t_1)} \quad (4)$$

$$m_c = \frac{276{,}030}{4{,}188.47 \cdot (25 - 5)} = 3.30\ kg/s$$

Step 7. Location of the fluids inside the heat exchanger:
According to suggestions stated by [2] and [20], the cold fluid (water) will be located inside of the inner tube, while the hot fluid (acetone) will flow on the annulus. Thus, the Table 4 presents the former and new symbols that will present the initial parameters for both fluids, taking into account the selected location of fluids. That is the subscripts h and c will be replaced by a and t, respectively, for all the initial parameters and physical properties of both fluids.

Table 4. Former and new symbols of the initial parameters for both fluids.

Parameter	Former symbol	New symbol	Units
Mass flowrate of acetone	m_h	m_a	kg/s
Mass flowrate of water	m_c	m_t	kg/s

Density of acetone	ρ_h	ρ_a	kg/m^3
Density of water	ρ_c	ρ_t	kg/m^3
Viscosity of acetone	μ_h	μ_a	Pa.s
Viscosity of water	μ_c	μ_t	Pa.s
Thermal conductivity of acetone	k_h	k_a	W/m.K
Thermal conductivity of water	k_c	k_t	W/m.K
Heat capacity of acetone	Cp_h	Cp_a	J/kg.K
Heat capacity of water	Cp_c	Cp_t	J/kg.K
Fouling factors of acetone	R_h	R_a	m^2.K/W
Fouling factors of water	R_c	R_t	m^2.K/W

Source: Own elaboration.

Table 5 exhibits the results of the parameters determined in steps 8 to 17.

Table 5. Results of the parameters determined in steps 8 – 17.

Step	Parameter	Symbol	Value	Units	Equat.
8	Net cross-sectional area in the annulus with longitudinal finned tubes	A_c	0.00129	m^2	(5)
9	Total wetted perimeter of the annulus with longitudinally finned inner tubes	P_w	0.949	m	(6)
10	Hydraulic diameter	D_h	0.0054	m	(7)
11	Heat transfer perimeter of the annulus for heat transfer	P_h	0.784	m	(8)
12	Equivalent diameter for heat transfer	D_e	0.0066	m	(9)
13	Velocity of the water	u_t	9.60	m/s	(10)
14	Reynolds number of the water[1]	Re_t	176,094	-	(11)
15	Prandtl number of the water	Pr_t	8.10	-	(12)
16	Friction factor	f_t	0.0040	-	(16)
	Nusselt number of the water	Nu_t	1,017.61	-	(17)
17	Convective heat transfer coefficient of the water	h_t	28,637	W/m^2.K	(18)

[1]Since Re_t > 10,000 the tube-side fluid flows under turbulent regime, thus equations (16) and (17) will be used to determine the Nusselt number.
Source: Own elaboration.

Table 6 exhibits the results of the parameters calculated in steps 18 to 22.

Table 6. Results of the parameters determined in steps 18 – 22.

Step	Parameter	Symbol	Value	Units	Equat.
18	Velocity of the acetone	u_a	2.08	m/s	(19)
19	Reynolds number of the acetone[1]	Re_a	36,550.6	-	(20)
20	Prandtl number of the acetone	Pr_a	3.61	-	(21)
	Friction factor	f_a	0.0056	-	(24)
21	Nusselt number of the acetone	Nu_a	186.69	-	(25)
22	Convective heat transfer coefficient of the acetone	h_a	4,127.6	W/m^2.K	(26)

[1]Since Re_a > 10,000 the annulus fluid flows under turbulent regime, thus equations (24) and (25) will be used to determine the Nusselt number.
Source: Own elaboration.

Table 7 shows the results of the parameters calculated in steps 23 to 36.

Table 7. Results of the parameters determined in steps 23 – 36.

Step	Parameter	Symbol	Value	Units	Equat.
23	Finned heat transfer area	A_f	6.092	m^2	(27)
24	Unfinned heat transfer area	A_u	0.492	m^2	(28)
25	Total area of hairpin	A_t	6.584	m^2	(29)
26	Factor	m	420	-	(30)
27	Fin efficiency	η_f	0.190	-	(31)
28	Overall surface efficiency	η_o	0.250	-	(32)
29	Area of the inner tube	A_i	0.552	m^2	(33)
30	Overall heat transfer coefficient (fouled)	U_f	182.65	W/m^2.K	(34)

31	Overall heat transfer coefficient (clean)	U_c	508.39	W/m^2.K	(35)
32	Cleanliness factor	CF	0.359	-	(36)
33	Log-mean temperature difference	$LMTD$	41.86	ºC	(37)
34	Total heat transfer surface area without fouling	A_{oc}	12.97	m^2	(38)
35	Total heat transfer surface area with fouling	A_{of}	36.10	m^2	(39)
36	Number of hairpins	N_h	2.78 ≈ 3	-	(40)

Source: Own elaboration.

3.2. Pressure drop.

Since the tube side fluid (water) flows under turbulent regime (Re_t = 176,094 > 10,000), the equations (43) and (44) were used to determine the pressure drop for this fluid. Accordingly:

Step 37. Friction factor of water (f_t') for turbulent regime:

$$f_t' = 0.00140 + 0.125 \cdot Re_t^{-0.32} = 0.0040 \quad (43)$$

Step 38. Pressure drop of water (Δp_t):

$$\Delta p_t = 4 \cdot f_t' \cdot \frac{2 \cdot L_t}{d_i} \cdot \rho_t \cdot \frac{u_t^2}{2} \cdot N_h = 886{,}903\ Pa \quad (44)$$

Because the annulus fluid (acetone) flows under turbulent regime (Re_a = 36,550.6 > 10,000), the equations (47) and (48) were used to determine the pressure drop for this fluid. Therefore:

Step 39. Friction factor of acetone (f_a') for turbulent regime:

$$f_a' = 0.00140 + 0.125 \cdot Re_a^{-0.32} = 0.0057 \quad (47)$$

Step 40. Pressure drop of acetone (Δp_a):

$$\Delta p_a = 4 \cdot f_a' \cdot \frac{2 \cdot L_t}{D_h} \cdot \rho_a \cdot \frac{u_a^2}{2} \cdot N_h = 171{,}518\ Pa \quad (48)$$

3.3. Pumping power.

Step 41. Pumping power required for the water (P_t):

$$P_t = \frac{m_t \cdot \Delta p_t}{\rho_t \cdot \eta_p} = 3{,}662\ W \quad (49)$$

Step 42. Pumping power required for the acetone (P_a):

$$P_a = \frac{m_a \cdot \Delta p_a}{\rho_a \cdot \eta_p} = 575\ W \quad (50)$$

4. Discussion.

The heat load necessary to cool down the acetone stream was of 276,030 W, while a mass flowrate of chilled water of 3.30 kg/s is needed by the heat exchange process. The velocity of chilled water (9.60 m/s) is 4.61 times higher than the velocity of acetone (2.08 m/s). This is because the higher value of the chilled water mass flowrate (3.30 kg/s) as compared to the mass flowrate of acetone (2.0 kg/s), as well as to the higher value of the parameter net cross-sectional area in the annulus with longitudinal finned tubes (0.00129 m^2) used in equation (19), as compared with the value of the term $\pi \cdot d_i / 4$ (0.00034 m^2) used in equation (10).

The Reynolds number of the chilled water (176,094) is about 4.82 times higher than the Reynolds number of acetone (36,550.6), which is due to the higher value of the velocity (9.60 m/s) and density (999.10 kg/m^3) of the chilled water compared to the values of these parameters for the acetone (velocity of 2.08 m/s and density of 745.20 kg/m^3). Also, the higher value obtained for the inner diameter of the tube (0.02093 m), as compared to the value of the hydraulic diameter (0.0054 m), influenced in this result. As stated above, the fluids will flow under turbulent regime inside the designed DPHE since the calculated values of the Reynolds number for both fluids are higher than 10,000.

In case of the Nusselt number, the value of this parameter for chilled water (1,017.61) is 5.45 times higher than the Nusselt number of acetone (186.69), which is due to the higher values obtained of Reynolds (176,094) and Prandtl (8.10) number for chilled water as compared to the values of this parameters for acetone (Reynolds number of 36,550.6 and Prandtl number of 3.61).

Regarding the convective heat transfer coefficient, the value of this parameter for the chilled water (28,637 W/m^2.K) is 6.94 times higher than the value obtained for the acetone. This is mainly due to the higher value of the Nusselt number (1,017.61) and thermal conductivity (0.589 W/m.K) obtained for chilled water as compared to the values of these parameters for acetone (Nusselt number of 186.69 and thermal conductivity of 0.146 W/m.K).

The calculated value of the fin efficiency was 0.190, which can be considered low. This is primarily due to the high value obtained for the convective heat transfer coefficient of acetone (4,127.6 W/m^2.K), which in turn increases the value of the factor m (equation 30) thus decreasing the fin efficiency (equation 31). The overall surface efficiency had a value of 0.250, which can also be considered low. The low value obtained for the fin efficiency influenced in the low value of the overall surface efficiency.

The overall heat transfer coefficient under clean conditions (U_c) had a value of 508.39 W/m^2.K, which is 2.78 times higher than the overall heat transfer coefficient under fouled conditions (182.65 W/m^2.K). The calculated value of U_c agrees with the ranges reported by [5] and [18] for this type of heat transfer service.

The cleanliness factor had a value of 0.359, which can be considered low. This is owing to the small value obtained

for the overall heat transfer coefficient under fouled conditions (182.65 W/m^2.K) and the high value of the clean surface overall heat transfer coefficient (508.39 W/m^2.K). The value of the cleanliness factor calculated in this study is lower than the value suggested by [5] for typical designs (0.85). According to [5], the cleanliness factor is a term developed for the steam power industry that provides an allowance for fouling and which relates the overall heat transfer coefficient when the heat exchanger is fouled to when it is clean. This approach provides a fouling allowance that varies directly with the clean surface overall heat transfer coefficient (U_c), and although the cleanliness factor results in favorable trends, the designer is still left with the problem of selecting the appropriate CF for his application [5].

The total heat transfer surface area with and without fouling had values of 36.10 m^2 and 12.97 m^2 respectively; therefore around 3 hairpins will be needed for the designed finned tube DPHE (Figure 3). The calculated values of the pressure drop for the chilled water and acetone were 886,903 Pa and 171,518 Pa, respectively, which are below the maximum allowable pressure drop values set by the process for both fluids (900,000 Pa and 200,000 Pa for chilled water and acetone respectively). It's worth mentioning that the pressure drop of chilled water is 5.17 times higher than the pressure drop of acetone, which is due essentially to the higher value obtained for the velocity (9.60 m/s) and density (999.10 kg/m^3) for chilled water as compared to the values obtained of these parameters for the acetone (velocity and density of 2.08 m/s and 745.20 kg/m^3 respectively).

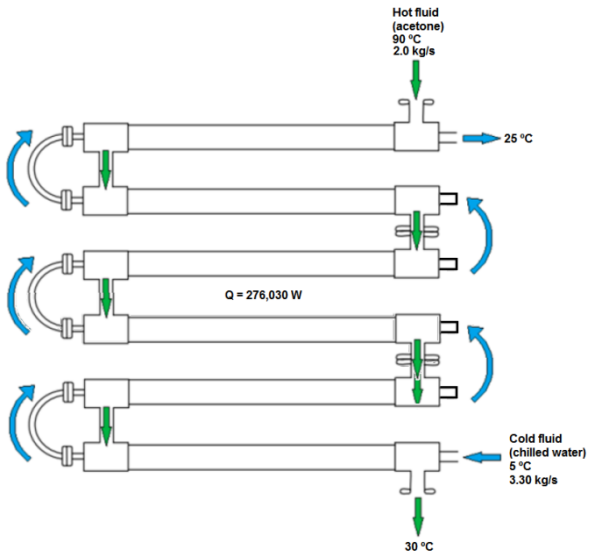

Fig. 3. Schematics of the designed finned tube DPHE containing the three hairpins and fluids flowing under countercurrent arrangement.
Source: Own elaboration.

Finally, the pumping power required for the chilled water (3,662 W) is 6.37 times higher than the pumping power required for acetone (575 W), which is largely due to the higher value of pressure drop obtained for the chilled water stream as compared to the value of pressure drop for acetone.

In [5], a finned tube DPHE was designed to cool 3 kg/s of a an engine oil stream from 65 ºC to 55 ºC using sea water available at 20 ºC, where the sea water (cold fluid) was located in the inner tube and the engine oil in the annulus. Among the results obtained, the flow regime in the inner tube is turbulent and in the annulus is laminar; the fin efficiency and overall surface efficiency have values of 0.682 and 0.703, respectively; the overall heat transfer coefficient under fouled and clean conditions are 108.6 W/m^2.K and 127.6 W/m^2.K, respectively; the cleanliness factor is 0.85 and two hairpins will be necessary for this heat transfer service. Finally, the pressure drop and pumping power for the sea water are 135 kPa and 237.3 W, respectively, while the pressure drop and pumping power for the engine oil (under laminar regime) are 7.5 MPa and 31.8 kW, respectively.

In [2] another finned tube DPHE was designed using the Kern's design methodology, where it is desired to cool 8,165 kg/h of 28 ºAPI gas oil from 121 ºC to 93 ºC using water at 27 ºC as the cooling medium. In this design project, the hot fluid (gas oil) was located in the annulus, while the cold fluid (water) was located in the inner tube. The values for the fin efficiency and the overall surface efficiency are 0.307 and 1.54, respectively; while the clean and the fouled (design) overall coefficients have values of 1,618.3 W/m^2.K and 670 W/m^2.K, respectively. It is necessary to use four hairpins and the calculated pressure drops in the annulus and inner pipe are of 62,604.39 Pa and 10,824.77 Pa, respectively.

5. Conclusions.

A finned-tube double-pipe heat exchanger was designed from both the thermal and hydraulic viewpoints using the methodology and correlations reported in [5] and [18], where several design parameters were determined such as cleanliness factor and the number of hairpins, as well as the pressure drop and pumping power of both streams, among others. The heat load had a value of 276,030 W, while a mass flowrate of chilled water of 3.30 kg/s will be needed to cool the acetone stream. Considering the calculated values of the Reynolds number for the chilled water (176,094) and acetone (36,550.6), both streams will flow under turbulent regime inside the designed DPHE, while the convective heat transfer coefficients for the chilled water and acetone were of 28,637 and 4,127.6 W/m^2.K, respectively. The overall heat transfer coefficient under fouled and clean conditions had values of 182.65 and 508.39 W/m^2.K, respectively, while the cleanliness factor was 0.359. The total heat transfer surface area without and with

fouling had values of 12.97 and 36.10 m^2, respectively. The designed finned tube DPHE will need three hairpins, and the pressure drop of both the chilled water (886,903 Pa) and acetone (171,518 Pa) are below the maximum values established by the heat exchange process. The chilled water stream will need a pumping power of 3,662 W, while the pumping power required by the acetone stream will be of 575 W.

6.- Author Contributions.

1. Conceptualization: Amaury Pérez Sánchez.
2. Data curation: Laura Thalía Alvarez Lores.
3. Formal Analysis: Amaury Pérez Sánchez, Elizabeth Elianne Artigas Cañizares.
4. Acquisition of funds: Not applicable.
5. Research: Amaury Pérez Sánchez, Elizabeth Elianne Artigas Cañizares, Laura Thalía Alvarez Lores.
6. Methodology: Amaury Pérez Sánchez.
7. Project management: Not applicable.
8. Resources: Not applicable.
9. Software: Not applicable.
10. Supervision: Amaury Pérez Sánchez.
11. Validation: Amaury Pérez Sánchez.
12. Visualization: Not applicable.
13. Writing – original draft: Elizabeth Elianne Artigas Cañizares, Laura Thalía Alvarez Lores
14. Writing - revision y editing: Amaury Pérez Sánchez.

7.- Referencias.

[1] K. S. Syed, M. Ishaq, Z. Iqbal, and A. Hassan, "Numerical study of an innovative design of a finned double-pipe heat exchanger with variable fin-tip thickness," *Energy Conversion and Management,* vol. 98, pp. 69-80, 2015. http://dx.doi.org/10.1016/j.enconman.2015.03.038

[2] M. Flynn, T. Akashige, and L. Theodore, *Kern's Process Heat Transfer*, 2nd ed. Beverly, USA: Scrivener Publishing, 2019.

[3] A. Faisal and S. Jain, "Analysis of a Double Pipe Heat Exchanger with Straight and Helical Fins," *International Journal of Science, Engineering and Technology,* vol. 9, no. 4, pp. 1-6, 2021.

[4] M. Ishaq, A. Ali, M. Amjad, K. S. Syed, and Z. Iqbal, "Diamond-Shaped Extended Fins for Heat Transfer Enhancement in a Double-Pipe Heat Exchanger: An Innovative Design," *Applied Sciences,* vol. 11, p. 5954, 2021. https://doi.org/10.3390/app11135954

[5] S. Kakaç, H. Liu, and A. Pramuanjaroenkij, *Heat Exchangers - Selection, Rating and Thermal Design*, 3rd ed. Boca Raton, USA: Taylor & Francis Group, 2012.

[6] Peccini, J. C. Lemos, A. L. H. Costa, and M. J. Bagajewicz, "Optimal Design of Double Pipe Heat Exchanger Structures," *Industrial & Engineering Chemistry Research,* vol. 58, p. 12080−12096, 2019. https://10.1021/acs.iecr.9b01536

[7] M. K. Alkam and M. A. Al-Nimr, "Improving the performance of double-pipe heat exchangers by using porous substrates," *International Journal of Heat and Mass Transfer,* vol. 42, pp. 3609-3618, 1999.

[8] M. F. Hasan, M. Danismaz, and B. M. Majel, "Thermal performance investigation of double pipe heat exchanger embedded with extended surfaces using nanofluid technique as enhancement," *Case Studies in Thermal Engineering,* vol. 43, p. 102774, 2023. https://doi.org/10.1016/j.csite.2023.102774

[9] Jalili, N. Aghaee, P. Jalili, and D. D. Ganji, "Novel usage of the curved rectangular fin on the heat transfer of a double-pipe heat exchanger with a nanofluid," *Case Studies in Thermal Engineering,* vol. 35, p. 102086, 2022. https://doi.org/10.1016/j.csite.2022.102086

[10] G. A. Rao and Y. Levy, "A semi empirical methodology for performance estimation of a double pipe finned heat exchanger," presented at the 9th Biennial ASME Conference on Engineering Systems Design and Analysis (ESDA08), Haifa, Israel, 2008.

[11] M. Sanchouli, S. Payan, A. Payan, and S. A. Nada, "Investigation of the enhancing thermal performance of phase change material in a double-tube heat exchanger using grid annular fins," *Case Studies in Thermal Engineering,* vol. 34, p. 101986, 2022. https://doi.org/10.1016/j.csite.2022.101986

[12] J. Mansour, Z. K. Kadhim, and K. A. Hussein, "CFD study of Heat Transfer Characteristics for Annular Serrated Finned-Tube Heat Exchanger," *Journal of Computer and Engineering Technology,* vol. 5, no. 1, pp. 77-87, 2018.

[13] V. Mathanraj, V. L. Krishna, J. L. V. Babu, and S. A. Kumar, "Experimental investigation on heat transfer in double pipe heat exchanger employing triangular fins," *IOP Conf. Series: Materials Science and Engineering,* vol. 402, p. 012137, 2018. https://doi.org/10.1088/1757-899X/402/1/012137

[14] S. Al-Zahrani, "Heat transfer characteristics of innovative configurations of double pipe heat exchanger," *Heat and Mass Transfer,* pp. 1-15, 2023. https://doi.org/10.1007/s00231-023-03360-0

[15] S. Sivalakshmi, M. Raja, and G. Gowtham, "Effect of helical fins on the performance of a double pipe heat exchanger," *Materials Today: Proceedings,* vol. 43, pp. 1128-1131, 2021. https://doi.org/10.1016/j.matpr.2020.08.563

[16] S. Kumar, K. V. Karanth, and K. Murthy, "Numerical study of heat transfer in a finned double pipe heat exchanger," *World Journal of Modelling and Simulation,* vol. 11, no. 1, pp. 43-54, 2015.

[17] H. Kahalerras and N. Targui, "Numerical analysis of heat transfer enhancement in a double pipe heat exchanger with porous fins," *International Journal of Numerical Methods for Heat & Fluid Flow,* vol. 18, no. 5, pp. 593-617, 2008. http://dx.doi.org/10.1108/09615530810879738

[18] E. Cao, "Heat transfer in process engineering," New York, USA: McGraw-Hill, 2010.

[19] W. Green and M. Z. Southard, *Perry's Chemical Engineers' Handbook*, 9th ed. New York, USA: McGraw-Hill Education, 2019.

[20] R. Sinnott and G. Towler, *Chemical Engineering Design*, 6th ed. Oxford, United Kingdom: Butterworth-Heinemann, 2020.

Nomenclature

A_c	Net cross-sectional area in the annulus with longitudinal finned tubes	m^2
A_f	Finned heat transfer area	m^2
A_i	Area of the inner tube	m^2
A_{oc}	Total heat transfer surface area without fouling	m^2
A_{of}	Total heat transfer surface area with fouling	m^2
A_t	Total area of hairpin	m^2
A_u	Unfinned heat transfer area	m^2
Cp	Heat capacity	J/kg.K
CF	Cleanliness factor	-
d_i	Inner diameter of tube	m
d_o	Outer diameter of tube	m
D_e	Equivalent diameter for heat transfer	m
D_h	Hydraulic diameter	m
D_i	Inner diameter of annulus	m
f	Friction factor for heat transfer	-
f'	Friction factor for pressure drop	-
h	Convective heat transfer coefficient	$W/m^2.K$
H_f	Fin height	m
k	Thermal conductivity	W/m.K

k_m	Thermal conductivity of the inner tube material	W/m.K
L_t	Length of hairpin	m
LMTD	Log-mean temperature difference	ºC
m	Mas flowrate	kg/s
m	Factor	-
N_f	Number of fins per tube	-
N_h	Number of hairpins	-
N_t	Number of tubes inside the annulus	-
Nu	Nusselt number	-
Δp	Pressure drop	Pa
Δp_m	Maximum allowable pressure drop	Pa
P	Pumping power	W
P_h	Heat transfer perimeter of the annulus for heat transfer	m
Pr	Prandtl number	-
P_w	Total wetted perimeter of the annulus with longitudinally finned inner tubes	m
Q	Heat load	W
R	Fouling factor	m^2.K/W
Re	Reynolds number	-
t	Temperature of the cold fluid	ºC
T	Temperature of the hot fluid	ºC
T_w	Tube wall temperature	ºC
$\bar{t}$	Average temperature of the cold fluid	ºC
$\overline{T}$	Average temperature of the hot fluid	ºC
u	Velocity	m/s
U_c	Overall heat transfer coefficient under clean conditions	W/m^2.K
U_f	Overall heat transfer coefficient under fouling conditions	W/m^2.K

Greek symbols

ρ	Density	kg/m^3
μ	Viscosity	Pa.s
δ	Fin thickness	m
η_f	Fin efficiency	-
η_o	Overall surface efficiency	-

Subscripts

1	Inlet
2	Outlet
c	Cold fluid
h	Hot fluid
a	Annulus fluid
t	Tube side fluid